

Article

Synthesis of an Electrodeficient Dipyridylbenzene-like Terdentate Ligand: Cyclometallating Ligand for Highly Emitting Iridium(III) and Platinum(II) Complexes

Pierre-Henri Lanoë * , Christian Philouze and Frédérique Loiseau *

CNRS, DCM, Univ. Grenoble Alpes, 38000 Grenoble, France; christian.philouze@univ-grenoble-alpes.fr

* Correspondence: pierre-henri.lanoë@univ-grenoble-alpes.fr (P.-H.L.); frederique.loiseau@univ-grenoble-alpes.fr (F.L.)

Abstract: Cyclometallated iridium(III) and platinum(II) complexes are intensely used in optoelectronics for their photophysical properties and ability to convert excitons from singlet to triplet state, thus improving the device efficiency. In this contribution, we report the multi-steps synthesis of an electrodeficient dipyridylbenzene-like terdentate ligand [N^C^N], namely 2',6'-dimethyl-2,3':5':2''-terpyridine (**6**), with 18% overall yield. Compound **6** has been employed to synthesize two phosphorescent complexes of platinum(II) and iridium(III), namely compounds **7** and **8**, respectively. Both complexes have been characterized by NMR and high resolution mass spectrometry, and demonstrate high luminescence quantum yields in a deaerated solution at room temperature, with 18% and 61% for **7** and **8**, respectively. If the iridium(III) complex displays similar emission properties to [Ir(dpyx)(ppy)Cl] (dpyx = 3,5-dimethyl-2,6-dipyridylbenzene and ppy = 2-phenylpyridine), the platinum(II) derivative, with $\lambda_{\text{em}} = 470$ nm, is a rare example of a fluorine atom-free blue emitting [N^C^N]PtCl complex.

Keywords: ligand synthesis; phosphorescence; platinum; iridium; blue emission; cyclometallating coordination



Citation: Lanoë, P.-H.; Philouze, C.; Loiseau, F. Synthesis of an Electrodeficient Dipyridylbenzene-like Terdentate Ligand: Cyclometallating Ligand for Highly Emitting Iridium(III) and Platinum(II) Complexes. *Organics* **2023**, *4*, 403–416. <https://doi.org/10.3390/org4030029>

Academic Editor: Adi Wolfson

Received: 2 May 2023

Revised: 30 May 2023

Accepted: 3 July 2023

Published: 14 July 2023



Copyright: © 2023 by the authors. Licensee MDPI, Basel, Switzerland. This article is an open access article distributed under the terms and conditions of the Creative Commons Attribution (CC BY) license (<https://creativecommons.org/licenses/by/4.0/>).

1. Introduction

Cyclometallated iridium(III) and platinum(II) complexes become cornerstones in modern photochemistry and find applications in optoelectronics, sensors, and luminescent biological probes for confocal microscopy, to name a few examples [1–13]. Cyclometallation means the formation of a bond between the metal and a carbon atom of a polydentate ligand, with the remaining bonds to the metal center usually being formed by heteroatoms such as nitrogen atoms. These complexes are thus organometallic compounds. The archetypical ligand being 2-phenylpyridine (ppy) reacts efficiently with Pt^{II} and Ir^{III} forming five-membered metallacycles, in which the carbon atom of the phenyl in the ortho of the linking pyridine is bound to the metal. The C–H activation generates a carbanion C[–], for which the σ donor ability is strong, while pyridine is a π acceptor. This ligand provides a very strong ligand-field to the metal, and thus the photophysical properties of the excited state are greatly enhanced. Indeed, in comparison with the polypyridines analogues, the strong ligand field uses high energy to push to a metal-centered (MC) excited state. This MC state is strongly coupled with the ground state and is thus responsible for the very low emission quantum yield when thermally accessible, such as in the case of Ru^{II}, Fe^{II}, and Os^{II} complexes [14,15]. These complexes' emission quantum yields are below 10%, with a few exceptions [15,16]. Therefore, it is not surprising that cyclometallated Ir^{III} and Pt^{II} complexes have been studied or are used in numerous applications, such as triplet emitters in electroluminescent devices [1–20], sensors [21–26], theragnostic and/or therapeutic agents [27–32], and photosensitizers and photocatalysts [13,21,33], to name few examples. The modification of the ligand framework around the metal center(s) allows for fine tuning their emission properties that cover the full visible spectra up to the near infrared [34–38].

Cyclometallated Ir^{III} complexes are usually encountered as part of one of the following three families: neutral trishomoleptic Ir(C⁺N)₃, where C⁺N is a cyclometallating ligand such asppy; neutral or cationic bis(heteroleptic) Ir(C⁺N)₂L, where L can be a monoanionic such as acetylacetone (acac) or a neutral bidentate such as bipyridine (bpy: 2'-bipyridine); or tris(heteroleptic) complexes with three different cyclometallating ligands [39,40], or of the form Ir(N⁺C⁺N)(C⁺N)Cl, where N⁺C⁺N is a terdentate such as bipyridylbenzene. The Pt^{II} complex counterparts, when limited to cyclometallating compounds, can be divided into four main families, namely: Pt(C⁺N)L, with the L ancillary ligand, which can be anionic (acac) or neutral (bpy); Pt(N⁺C⁺N)X; the isoelectronic Pt(C⁺N⁺N)X; and Pt(C⁺N⁺C)X (X: halogen, thiocyanate, etc.).

Efficient blue emitting phosphors are still challenging to accomplish because of the high energy gap needed between the triplet excited state and the singlet ground state. To date, the main strategy for obtaining blue emitting Pt^{II} and Ir^{III} complexes is to introduce fluorine atoms or fluorinated substituents onto the ligand framework [34,35,41]; recent work achieved deep blue emitting complexes by using the biscarbene pincer ligand, isoelectronic to the N⁺C⁺N ligand [42–44]. However, in electroluminescent devices, the presence of fluorine atoms directly attached to aromatic carbons on the ligand framework is thought to lead to decomposition of the complex [45]. The only fluorine atom-free blue emitting Pt(N⁺C⁺N)Cl complex had an ester in the *para* position of the cyclometallating benzene with respect to the C-Pt bond, and it displayed a high photoluminescent quantum yield of 58% and an emission maximum at 481 nm in CH₂Cl₂ at 298 K [46]. A recent strategy was to introduce an electrodeficient cyclometallating aryl such as pyrimidine, or to destabilize the LUMO by using an electron rich ancillary ligand and donor substituents [47–49]. In this contribution, we focus especially on the Ir^{III} and Pt^{II} complexes featuring a terdentate ligand N⁺C⁺N, namely 2',6'-dimethyl-2,3':5',2''-terpyridine (**6**). This ligand, although a substituted terpyridine, behaves as its structural analogue 3,5-dimethyl-2,6-dipyridylbenzene (=dpyxH) when it is coordinated to a metal center. Indeed, on ligand **6**, the presence of the methyl groups prevents the competitive coordination of the nitrogen atom of the central pyridine, promoting the cyclometallation on C4 just like with dpyxH. The complexes featuring the dpyx ligand are closely related to the position isomer C⁺N⁺N (6-phenyl-2,2'-bipyridine) [50], but the switch of position of the σ donor carbon has quite a dramatic effect on the luminescence properties. Both Pt(N⁺C⁺N)Cl and Ir(N⁺C⁺N)(C⁺N)Cl complexes display high emission quantum yields, which can almost reach unity in homo-bimetallic assemblies [51–53]. We depict the synthesis of a new electrodeficient cyclometallating ligand, namely 2',6'-dimethyl-2,3':5',2''-terpyridine (**6**), which, once coordinated to a platinum(II) center, allows for reaching blue emission.

2. Materials and Methods

2.1. General Consideration

Commercially available reagents were purchased from Sigma-Aldrich, Alfa Aesar, Acros Organics, TCI Chemical, Merck, Strem, or Fluorochem and used as received, unless otherwise specified. Solvents were obtained from same commercial sources and used without further purification. For moisture sensitive reactions, glassware was oven-dried prior to use. ¹H NMR spectra were recorded on a Brucker advance III 400 MHz spectrometer equipped with a BBO probe and on a Brucker advance III 500 MHz spectrometer equipped with a CryoProbe Prodigy in deuterated solvent (CDCl₃, DMSO-d₆ or CD₂Cl₂) and data were reported as follows: chemical shift in ppm from tetramethylsilane with the solvent as an internal indicator (CDCl₃ 7.26 ppm, DMSO-d₆ 2.50 ppm, CD₂Cl₂ 5.32 ppm), multiplicity (s = singlet, d = doublet, t = triplet, q = quartet, p = pentet, m = multiplet or overlap of non-equivalent resonances), integration. ¹³C{¹H} NMR spectra were recorded either at 101 MHz or at 126 MHz in a suitable deuterated solvent and data are reported as follows: chemical shift in ppm from tetramethylsilane with the solvent as an internal indicator (CDCl₃ 77.16 ppm, DMSO-d₆ 39.52 ppm, CD₂Cl₂ 53.84 ppm). All NMR spectra are displayed in SI Figures S1–S11. High resolution mass spectrometry (HRMS) was performed on a THERMO

SCIENTIFIC LTQ Orbitrap XL in electrospray ionization (ESI) mode with a dilution of 10^{-5} M in MeOH.

2.2. Absorption and Emission Spectroscopies

The absorption spectra were recorded on a Cary 300 UV–visible spectrophotometer (Varian) and the emission spectra (in solution and at 77 K) were recorded on a Fluoromax 4® (Horiba) or on a FLS-1000® (Edinburgh Instruments) equipped with automatic filters to remove the harmonic bands. Quartz cuvettes with a 1 cm optical path were used. Lifetimes were measured using LP900 spectrometer with a Flashlamp pumped Q-switched Nd:Yag laser operating at 355 nm and with photomultiplier (PMT) detector, or with a picosecond laser diode operating at 405 nm and using a time-correlated single photon counting detection (TCSPC, PicoHarp 300). Phosphorescence quantum yields Φ were measured in diluted solutions with an optical density lower than 0.1, using the relative method (comparison with a reference compound, here diphenylanthracene in cyclohexane, $\Phi_r = 0.90$), according the following general equation: $\Phi_x/\Phi_r = [Ar/Ax][nx^2/nr^2][Dx/Dr]$, where A is the absorbance at the excitation wavelength, n the refractive index, and D the integrated luminescence intensity. “r” and “x” stand for reference and sample, respectively [54].

2.3. Experimental Procedures

2,6-dimethyl-4-pyridone (1): to 2,6-dimethyl- γ -pyrone (2 g, 16.11 mmol) in an Ace® tube was added to an aqueous solution of NH₄OH (8 mL, 25% w/w). The tube was sealed and the solution was stirred at 140 °C overnight. At r.t., the white precipitate was filtered out and washed with cold water. The pure compound was dried with P₂O₅ under reduced pressure, giving the desired product in 60% yield (1.18 g). ¹H NMR (400 MHz, DMSO-d₆) δ 11.08 (s, 1H), 5.75 (s, 2H), and 2.11 (s, 6H). The spectrum was coherent with the previously reported synthesis [55].

3,5-dibromo-2,6-dimethyl-4-pyridone (2): In an ice bath, **1** (2.5 g, 20.3 mmol) was suspended in dist. water (50 mL), followed by the addition of KOH (2.3 g, 40.6 mmol). Using a dropping funnel, Br₂ (12.4 g, 77.49 mmol) was added drop-to-drop, allowing the solution to lose the brown color and take the appearance of a white precipitate. After full addition, the suspension was stirred for 1h and the precipitate was collected on a frit. The cake was washed with water until the filtrate was colorless, then it was washed with cold methanol (30 mL) and cold diethylether (30 mL). The white solid was then dried in vacuum with P₂O₅ overnight. The compound was recovered as a white solid in 68% yield (6.77 g). ¹H NMR (400 MHz, CDCl₃) δ 6.94 (s, 1H) and 2.56 (s, 6H). The spectrum was coherent with the previously reported synthesis [55].

3,5-dibromo-4-chloro-2,6-dimethyl-4-pyridine (3): **2** (4 g, 14.3 mmol) and POCl₃ (16 mL, 78.4 mmol) were placed in a sealed tube (Ace® tube) and heated at 135 °C overnight. At r.t., the mixture was poured into ice and NaHCO₃ was added until neutralization of the pH. The aqueous phase was extracted three times with CH₂Cl₂ (50 mL) and the collected organic layers were dried on MgSO₄ and the solvent was evaporated. The crude product was purified using a flash chromatography column (SiO₂, C₆H₁₂/EtOAc/CH₃C₆H₅, 7/2.99/0.01, V/V/V) and the pure compound was obtained in a 73% yield (3.15 g). ¹H NMR (400 MHz, CDCl₃) δ 2.66 (s, 6H). The spectrum was coherent with the previously reported synthesis [55].

3,5-dibromo-2,6-dimethyl-4-pyridine (4): **3** (5 g, 16.59 mmol) was suspended in hydroiodic acid (57%, 25 mL) and red phosphorus (514 mg, 166 mmol) was added. The mixture was refluxed overnight. At r.t., the mixture was carefully added to a saturated solution of Na₂CO₃ (200 mL) and the mixture was extracted three times with CH₂Cl₂ (50 mL). The combined organic layers were dried over MgSO₄ and the solvents were evaporated. A flash chromatography column (SiO₂, C₆H₁₂/EtOAc, 6/4) produced the compound in 68% yield (3.01 g). ¹H NMR (400 MHz, CDCl₃) δ 6.60 (s, 1H), 2.07 (s, 6H). The spectrum was coherent with the previously reported synthesis [55].

3-bromo-5-phenyl-2,6-dimethyl-4-pyridine (5): **4** (1.44 g, 5.4 mmol), 2-(tributylstannyl)pyridine (5 g, 13.6 mmol) and anhydrous LiCl (1.67 g, 39 mmol) were dissolved/suspended in toluene (40 mL). The solution was degassed by bubbling Ar at the mean of a needle for 15–20 min, followed by the addition of Pd(PPh₃)₄ (254 mg, 0.22 mmol) and the solution was heated under reflux for 24 h. At room temperature, the solution was filtered on celite® and washed with toluene until the filtrate became colorless. After evaporation of the solvent, the crude material was purified by a flash chromatography column (SiO₂, pentane/dry-acetone, 6/4 to 4/6), producing two products: **5** in 65% yield (1 g) and 2,6-dimethyl-3,5-diphenyl-4-pyridine (**6**) in 24% yield (583 mg). ¹H NMR (400 MHz, CDCl₃) δ 7.65 (s, 1H), 7.48–7.33 (m, 3H), 7.29 (dd, *J* = 8.3 Hz, *J* = 1.6 Hz, 2H), 7.16 (ddd, *J* = 6.3 Hz, *J* = 0.9 Hz, 1H), 6.95 (ddd, *J* = 7.7 Hz, *J* = 1.7 Hz, 1H), 2.67 (s, 3H), 2.43 (s, 3H). ¹³C NMR (101 MHz, CDCl₃) δ 155.19, 154.02, 140.62, 138.66, 136.23, 129.87, 129.26, 129.08, 128.61, 127.99, 127.86, 127.68, 118.32, 24.63. HRMS calculated for [M + H]⁺ 263.01639, found 263.02546.

2',6'-dimethyl-2,3':5':2''-terpyridine (6) from **5**: **5** (1 g, 3.8 mmol), 2-(tributylstannyl)pyridine (1.8 g, 4.9 mmol) and anhydrous LiCl (590 mg, 39 mmol) were dissolved/suspended in toluene (30 mL). The solution was degassed by bubbling Ar at the mean of a needle for 15–20 min prior to the addition of Pd(PPh₃)₄ (175 mg, 0.15 mmol) and the solution was refluxed overnight. At room temperature, the solution was filtered on celite® and washed with toluene until the filtrate became colorless. After evaporation of the solvent, the crude material was purified by a flash chromatography column (SiO₂, pentane/dry-acetone, 6/4 to 4/6) giving **6** in 45% yield (443 mg). ¹H NMR (400 MHz, CD₂Cl₂) δ 8.69 (ddd, *J* = 4.9, 1.9, 1.0 Hz, 2H, 11), 7.84–7.73 (m, 3H, 12 & 4), 7.48 (dt, *J* = 7.8 Hz, *J* = 1.1 Hz, 2H, 13), 7.28 (ddd, *J* = 7.6 Hz, *J* = 4.8 Hz, *J* = 1.1 Hz, 2H, 14), 2.61 (s, 6H, 7 & 8). ¹³C NMR (101 MHz, CD₂Cl₂) {¹H} δ 158.4, 155.4, 149.9, 138.9, 136.7, 133.5, 124.4, 122.4, 23.4. HRMS calculated for [M + H]⁺ 262.13387, found 262.13358.

2',6'-dimethyl-2,3':5':2''-terpyridine (6) from **4**: **4** (350 g, 1.32 mmol), 2-(tributylstannyl)pyridine (1.5 g, 1.96 mmol) and anhydrous LiCl (348 mg, 15.3 mmol) were dissolved/suspended in toluene (20 mL). The solution was degassed by bubbling Ar at the mean of a needle for 15–20 min prior to the addition of Pd(PPh₃)₄ (100 mg, 0.09 mmol) and the solution was refluxed for 72 h under Ar. At room temperature, the solution was filtered on celite® and washed with toluene until the filtrate became colorless. After evaporation of the solvent, the crude material was purified by a flash chromatography column (SiO₂, ethylacetate), producing **6** in 87% yield (300 mg). ¹H NMR (400 MHz, CD₂Cl₂) δ 8.69 (ddd, *J* = 4.9, 1.9, 1.0 Hz, 2H, 11), 7.84–7.73 (m, 3H), 7.48 (dt, *J* = 7.8 Hz, *J* = 1.1 Hz, 2H), 7.28 (ddd, *J* = 7.6 Hz, *J* = 4.8 Hz, *J* = 1.1 Hz, 2H), 2.61 (s, 6H).

Compound **7**: **6** (100 mg, 0.38 mmol) and K₂PtCl₄ (157 mg, 0.38 mmol) were dissolved in a mixture of butyronitrile (15 mL) and H₂O (0.5 mL), and the reaction was refluxed for 60 h. At room temperature, the yellowish suspension was filtered on celite. The celite was recovered and suspended in 2-ethoxyethanol (20 mL) and refluxed 24 h. At room temperature, water was added (30 mL) and the suspension was filtered on celite. The celite was washed successively with ice-cold MeOH (20 mL) and Et₂O (30 mL). The celite was then treated with hot CH₂Cl₂ (3 × 10 mL) and hot MeNO₂ (3 × 10 mL). The combined organic phases were dried with MgSO₄, filtered, and evaporated under reduced pressure. Complex **7** was isolated as a pale yellow to red solid in 21% yield (40 mg). ¹H NMR (400 MHz, CD₂Cl₂) δ 9.41 (dd, *J*_{Pt-H} = 41.2 Hz, *J* = 5.7 Hz, 2H), 8.03 (t, *J* = 7.9 Hz, 2H), 7.94–7.82 (m, 2H), 7.34 (dd, *J* = 6.5 Hz, *J* = 6.5 Hz, 2H), 2.82 (s, 6H). The complex was not soluble enough to obtain the ¹³C NMR spectrum in CD₂Cl₂, nor CD₃Cl or DMSO-d₆. HRMS calculated for [M-Cl]⁺ 455.0835, found 455.0827; calculated for [M-Cl + CH₃CN]⁺ 496.1101, found 496.1066.

Compound **8**: **6** (80 mg, 0.31 mmol) and IrCl₃·H₂O (88 mg, 0.30 mmol) were dissolved in a mixture of 2-ethoxyethanol/H₂O (20 mL, 3/1, *v/v*) and refluxed overnight. At room temperature, H₂O was added until precipitation, and the solid was then filtered on Milipore and copiously washed with H₂O and Et₂O. The crude materials were suspended in toluene (5 mL) and 2-tolylpyridine (61 mg, 0.36 mmol) and AgOTf (128 mg, 0.5 mmol)

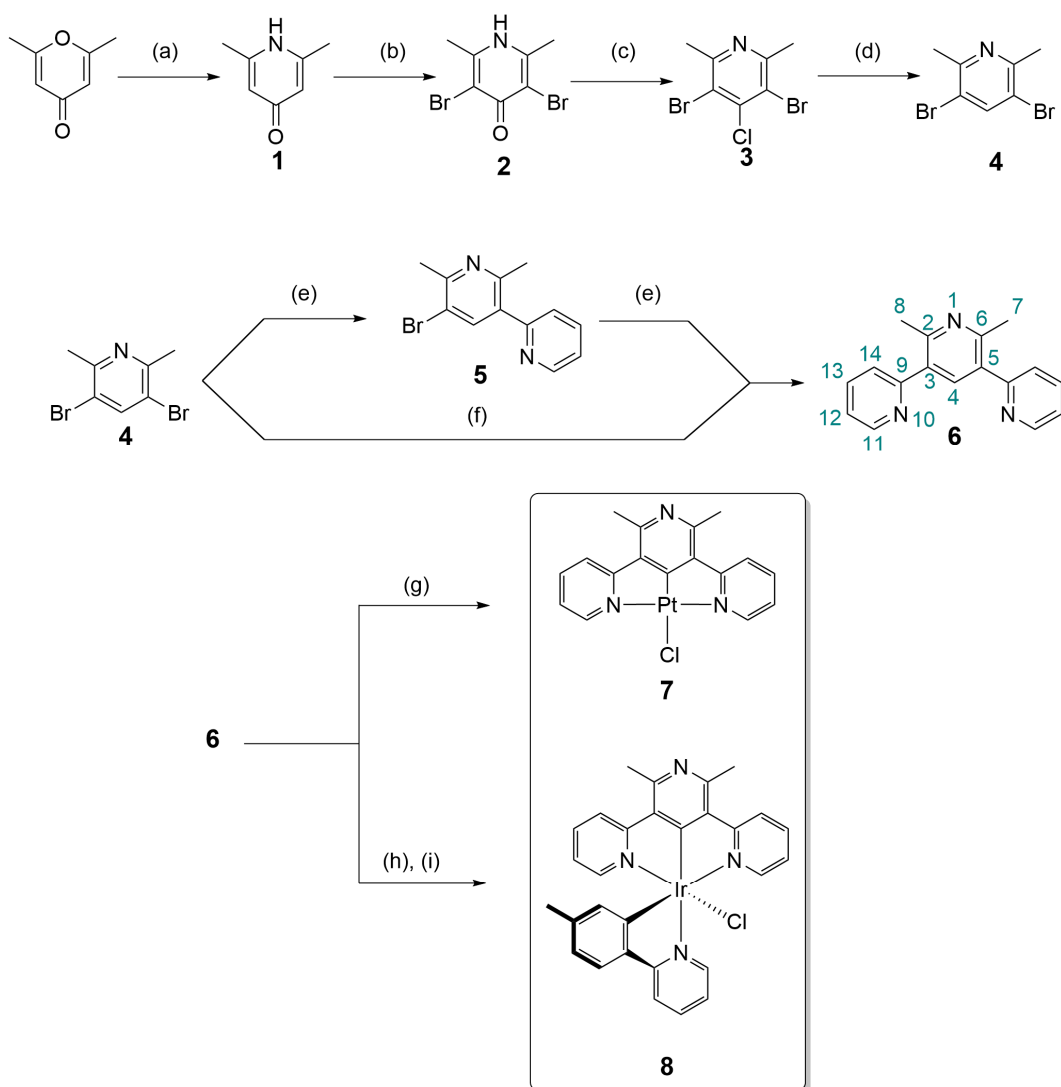
were added. The reaction was heated at reflux overnight. After evaporation of the solvent, the residue was suspended in CH_2Cl_2 and filtered on celite. The yellow solution was concentrated and an excess of Et_2O (roughly 2 or 3 \times the CH_2Cl_2 residual volume) and the solution stood in a freezer overnight. A yellow precipitate appeared and was filtrated on Millipore, washed with Et_2O , and the resulting solid was dried in a vacuum. The compound was isolated as a yellow powder in 61% yield (128 mg). ^1H NMR (500 MHz, CD_2Cl_2) δ 9.99 (ddd, $J = 5.5, 1.7, 0.9$ Hz, 1H), 8.08 (ddd, $J = 8.7, 2.4, 1.2$ Hz, 3H), 8.04–7.97 (m, 1H), 7.76–7.68 (m, 4H), 7.57 (ddd, $J = 7.2, 5.5, 1.4$ Hz, 1H), 7.52 (d, $J = 7.9$ Hz, 1H), 6.94 (ddd, $J = 7.2, 5.8, 1.4$ Hz, 2H), 6.57 (ddd, $J = 7.9, 1.8, 0.8$ Hz, 1H), 5.69 (d, $J = 1.8$ Hz, 1H), 3.76 (s, 2H), 3.06 (s, 6H). ^{13}C NMR (126 MHz, CD_2Cl_2) δ 167.64, 164.62, 152.04, 149.40, 146.19, 141.13, 139.99, 138.31, 137.25, 136.59, 135.47, 124.41, 123.48, 123.04, 122.96, 119.27, 54.27, 54.06, 53.84, 53.62, 53.41, 44.34, 21.37. HRMS calculated for $[\text{M}-\text{Cl}]^+$ 621.16302, found 621.16171.

3. Results

3.1. Synthesis

The synthesis of the dipyridylbenzene-like terdentate ligand **6** (Scheme 1) was adapted from known procedures [55,56] and started from the conversion of 2,6-dimethyl- γ -pyrone into 2,6-dimethyl-4-pyridone (**1**) in a pressure tube in the presence of an excess ammonia aqueous solution at a high temperature, with a moderate conversion yield (60%). The dibromopyridone **2** was obtained through the addition of bromine to an alkaline solution of compound **1**, which provided access to the desired derivative in a moderate yield (68%). The aromatization and conversion of compound **2** to **3** was performed in neat phosphoryl chloride at a high temperature in a pressure tube. After neutralization of the reaction mixture and extraction, the desired compound **3** was obtained after flash chromatography column in good yields (73%). The reduction in the chlorine atom was performed in a refluxing hydroiodic acid in the presence of red phosphorus and the subsequent neutralization and extraction gave a crude material. The latter was purified by a flash chromatography column, yielding **4** (65%). To our surprise, the direct conversion of **4** to **6** by the Stille palladium cross-coupling reaction appeared to be somewhat slow. Indeed, the 1,5-dimethyl-3,4-di(2'-pyridyl)benzene synthesis in similar conditions [56] was obtained after 24 h of reaction in a moderate yield (61%) from the corresponding 1,5-dibromo-2,4-dimethylbenzene. In our case, when the work up of the reaction was performed after 24 h, the column chromatography allowed for isolating two compounds, the first eluted compound was the monosubstituted derivative **5** and the second one was compound **6**, in 65% and 24% yields respectively. A second cross-coupling reaction with **5** provided access to **6** in 45% yield, after purification. The direct access to the desired ligand through the cross-coupling reaction required three days of reflux with a slight increase in the Pd^0 load, 7% instead of 4%. The ligand was obtained in a high yield (87%) after column chromatography. When performing the cyclometallation reaction to afford complex **7** from the refluxing solution of **6** and K_2PtCl_4 in a different set of solvents acetic acid, or 2-ethoxyethanol, or in a mixture of solvents ($\text{CH}_3\text{COOH}/\text{CH}_3\text{CN}$), only degradation materials or starting ligands were observed. Therefore, we attempted the *in situ* formation of a bis(butynonitrile)dichloridoplatinum(II) complex that would react with ligand **6** [57]. After 60 h of reflux of a mixture of ligand **6** and K_2PtCl_4 in butyronitrile, the reaction was filtered, and the filtrate was free of materials and the celite displayed a pale yellow color. No product was recovered after washing the celite with hot CH_2Cl_2 . We presumed that the cyclometallation did not take place and the celite was refluxed for 24 h in 2-ethoxyethanol to allow for the cyclometallation to take place. After filtration and washing of the solid, the pure compound was obtained by treating the celite with hot CH_2Cl_2 and CH_3NO_2 , as a pale yellow to red solid in a low yield (21%). It is worth noting that the presence of a red color, along with a red emission, is characteristic of Pt–Pt interactions in the ground state in this family of square planar complexes [58]. The synthesis of complex **8** followed the classical two steps route [37,56]; first, ligand **6** was dissolved with $\text{Ir}^{\text{III}}\text{Cl}_3 \cdot n\text{H}_2\text{O}$ salt in a mixture

of ethoxyethanol/water and refluxed overnight, leading to a μ -dichlorobriged dimer. The latter was not characterized, which is somewhat common regarding the low solubility of these intermediates [37,56] and their known lack of interesting emission properties [59–61]. Thus, the intermediate was directly engaged in the next step and suspended in toluene in the presence of an excess of both 2-tolylpyridine and silver triflate. The mixture was refluxed overnight, and the workup followed by a recrystallisation provided the desired complex in a good yield (61%).



Scheme 1. Synthesis of compounds **1** to **8** (see H atoms numbering on **6**). (a) NH_4OH 140°C ; (b) Br_2 , KOH , H_2O ; (c) POCl_3 135°C ; (d) red phosphorus, HI_{aq} reflux; (e) 2-(tributylstannylyl)pyridine $\text{Pd}(\text{PPh}_3)_4$ (4 %mol), LiCl , toluene, Ar, reflux; (f) 2-(tributylstannylyl)pyridine $\text{Pd}(\text{PPh}_3)_4$ (7 %mol), LiCl , toluene, Ar, reflux; (g) K_2PtCl_4 $\text{ACOH}/\text{CH}_3\text{CN}$ reflux 24 h; (h) $\text{IrCl}_3 \cdot \text{nH}_2\text{O}$ 2-ethoxyethanol H_2O reflux; (i) 2-(tolyl)pyridine, AgOTf , toluene reflux, Ar;

3.2. Characterisation

The ^1H NMR spectrum of **7** displays four sets of multiplets in the aromatic region (Figure 1), of 9.5 ppm to 7.3 ppm, and a singlet in the aliphatic region. The latter corresponds to the methyl of the cyclometallating ring (6H) and the multiplets belong to the two coordinating pyridyls (8H). The presence of Pt^{II} was assessed by the strong coupling constant between the ^{195}Pt and the proton (Figure 1) with $J = 41.2$ Hz. It was not possible to record a proper ^{13}C NMR spectrum for the complex despite our efforts, notably by changing the solvent. The square planar Pt^{II} compounds are prone to interact, which can

obstruct their solubility, in contrast with the octahedral geometry of Ir^{III} complexes, which are consequently more soluble.

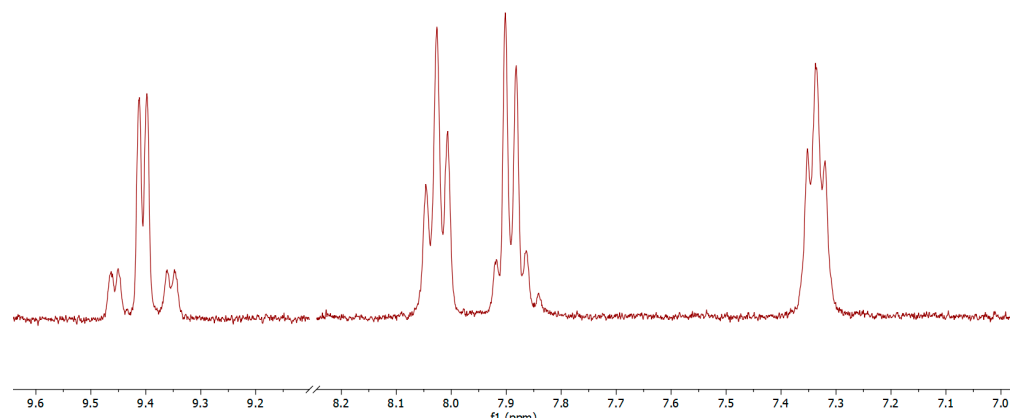


Figure 1. Complex 7, ^1H NMR spectrum of the aromatic region in CD_2Cl_2 , 400 MHz.

The ^1H NMR spectrum of **8** displayed nine signals belonging to the aromatic protons in the range of 5.5–10 ppm (Figure S11), counting for 15 protons. The doublet at 5.69 ppm corresponds to the proton in *ortho* position of the cyclometallating carbon of the tolylpyridine ligand, which is in the magnetic field of the $\text{N}^\text{C}\text{N}$ ligand. As a consequence, the chemical shift moved to a high field. Two singlets in the aliphatic region correspond to the methyl groups of both cyclometallating ligands. The NMR spectrum displays the expected number of protons.

3.3. X-ray Single Crystal Diffraction

Crystallographic quality crystals were obtained for **8** by slow vapor diffusion of *n*-hexane in a concentrated solution of the complex in 1,2-dichloroethane. The structure is shown in Figure 2. Compound **8** crystallizes in the triclinic space group P-1 with one complex per asymmetric unit. A selection of structural data are gathered in Table 1 and the crystal data and structure refinement are shown in Table S1. The geometrical constraints induced by the chelation of the terdentate ligand forming five member cycles lead to a distorted octahedral geometry coordination around the metal center, with an $\text{N}^\text{NCN}^\text{-}\text{Ir}^\text{-}\text{N}^\text{NCN}$ angle of 160.5° . The metal–ligand bonds are longer for the bidentate ligand than for the terdentate one, $\text{Ir}-\text{C}^\text{NCN}$ is $1.919(9)$ Å and the $\text{Ir}-\text{C}^\text{NC}$ is $2.019(6)$ Å; such a difference could be the result of the hindrance of the two flanking pyridyl rings of $\text{N}^\text{C}\text{N}$ ligand on the other ligand. $\text{Ir}-\text{N}^\text{NC}$ is $2.160(7)$ Å, longer than the other $\text{Ir}-\text{N}$ bonds, which display bond length of roughly 2.05 Å. This difference reflects the *trans* effect induced by the strong σ donating ability of the cyclometallating carbon. These values are similar to the one encountered in other iridium(III) complexes featuring the cyclometallating terdentate ligand [56,62,63].

3.4. Absorption and Emission Spectroscopy

The complexes were studied in a diluted solution of CH_2Cl_2 at 298 K under both air equilibrated and deaerated conditions, and at a low temperature (77 K) in a butyronitrile rigid matrix. The complexes $[\text{Pt}(\text{dpyx})\text{Cl}]$ [64] and $[\text{Ir}(\text{dpyx})(\text{ppy})\text{Cl}]$ [57] (dpyx = 3,5-dimethyl-2,6-dipyridylbenzene; and ppy = 2-phenylpyridine), presented in Figure 3, are structural analogues of **7** and **8** and were chosen as reference compounds for the study of the photophysical properties. A selection of data are gathered in Table 2 and the spectra are displayed in Figure 4. First, the compound **7** absorption spectrum displays intense bands in the 250–300 nm region ($\epsilon_{\text{max}} = 75,500 \text{ M}^{-1} \text{ cm}^{-1}$) and these bands are usually ascribed to the $\pi-\pi^*$ transitions of the ligand. Moderately intense absorption bands are present within the range of 300–390 nm with an average ϵ of $30,000 \text{ M}^{-1} \text{ cm}^{-1}$, they could be mixtures of metal perturbated ligand centered (LC) and metal-to-ligand charge transfer (MLCT)

transitions [58,65]. At low energy, a very weak absorption band is observed (440 nm, $\sim 800 \text{ M}^{-1} \text{ cm}^{-1}$, see Figure S12) and it can be ascribed to the direct absorption from the singlet ground state to the triplet excited state, which is partially allowed by the strong spin–orbit coupling of the platinum [58,65]. The shape of the spectrum is similar to the one displayed by $[\text{Pt}(\text{dpyx})\text{Cl}]$ [64], but the whole spectrum displays an hypsochromic shift, which could be the consequence of the use of the cyclometallating pyridine as expected. Second, compound **8** absorption spectrum displays relatively intense absorption band at 280 nm ($\epsilon = 34,500 \text{ M}^{-1} \text{ cm}^{-1}$) ascribed to the $\pi-\pi^*$ transitions centered on the ligands ($\text{N}^{\text{C}}\text{N}$ or/and C^{N}). In the range of 340–450 nm, the complex displays moderate absorption bands ($\epsilon = 6\,000\text{--}7\,500 \text{ M}^{-1} \text{ cm}^{-1}$), with no counterpart in the free ligands, which involve metal perturbated ligand transition with, at a lower energy, metal-to-ligand charge transfer (MLCT) and ligand–ligand charge transfer (LLCT) transitions [61,66]. At a low energy, a very weak absorption band around 480 nm ($\epsilon < 1\,000 \text{ M}^{-1} \text{ cm}^{-1}$, see Figure S12) corresponds to the direct absorption of the singlet ground state to the triplet excited state, which is partially allowed thanks to the high spin–orbit coupling brought by the Ir^{III} core [61,66].

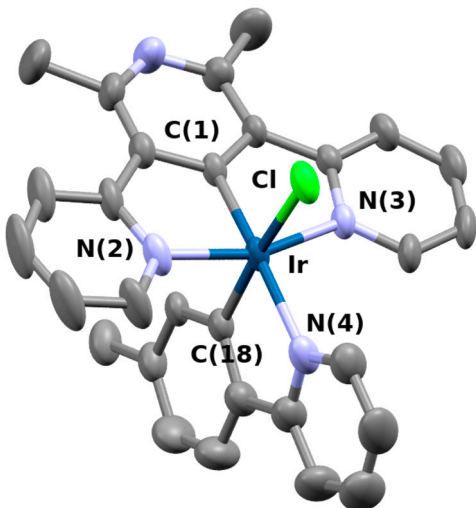


Figure 2. Molecular structure of **8**. Hydrogen atoms have been omitted for clarity.

Table 1. Selected structural data of **8**.

	Bond Length (Å)	Angles (°)	
Ir–C(1)	1.921(6)	C(1)–Ir–N(2)	80.4(2)
Ir–N(2)	2.043(6)	C(1)–Ir–N(3)	80.0(2)
Ir–N(3)	2.053(5)	C(1)–Ir–N(4)	174.2(2)
Ir–N(4)	2.158(5)	C(1)–Ir–C(18)	94.8(2)
Ir–C(18)	2.005(4)	C(1)–Ir–Cl	92.7(2)
Ir–Cl	2.462(2)	N(3)–Ir–C1	91.5(1)
		N(2)–Ir–C1	88.1(1)
		N(4)–Ir–Cl	93.0(1)
		C(18)–Ir–Cl	172.1(1)
		N(2)–Ir–N(3)	160.3(2)

At room temperature in a deaerated solution, compound **7** displays a structured blue-green emission with a maximum at 470 nm and a moderate quantum yield of 18%. The emission lifetime is of the μs regime (1.6 μs) and both the quantum yield and the lifetime drop slightly in the presence of oxygen with a moderate bimolecular quenching constant ($k[\text{O}_2] = 0.2\,10^{-9} \text{ M}^{-1} \text{ s}^{-1}$) [56,63,67]. The emission quantum yield of **7** is smaller than that of the model complex $[\text{Pt}(\text{dpyx})\text{Cl}]$ [64], with 18% and 49%, respectively. The introduction of a nitrogen atom in the cyclometallating aryl in the 4 position has the expected consequence

of inducing a strong hypsochromic shift, just like the presence of fluorine atoms in 3,5-position of the cyclometallating benzene in complex $[\text{Pt}(3,5\text{-dFdpb})\text{Cl}]$ (3,5-dFdpb = 3,5-difluoro-2,6-di(2-pyridyl)benzene, metallated at C1 of the benzene), which displays a structured emission with a maximum at 467 nm with a quantum yield of 80% in deaerated CH_2Cl_2 [34]. Complex 7 is one of the rare examples of the Pt(II) complex displaying a blue emission without the presence of fluorine substituents on the ligands. Such a result is impressive, as it is worth noting that the presence of F-C_{Ar} in the ligand framework is thought to induce degradation in electroluminescent devices [45]. At 77 K in a rigid matrix, the complex displays a slight bathochromic shift with a maximum emission at 463 nm and an extended emission lifetime of 2.3 μs . The weak rigidochromism displayed by 7, along with the relatively long emission lifetime, are indicative of an emission emanating from the radiative deactivation from the ligand centered (IL) triplet excited state to the singlet ground state [15,52].

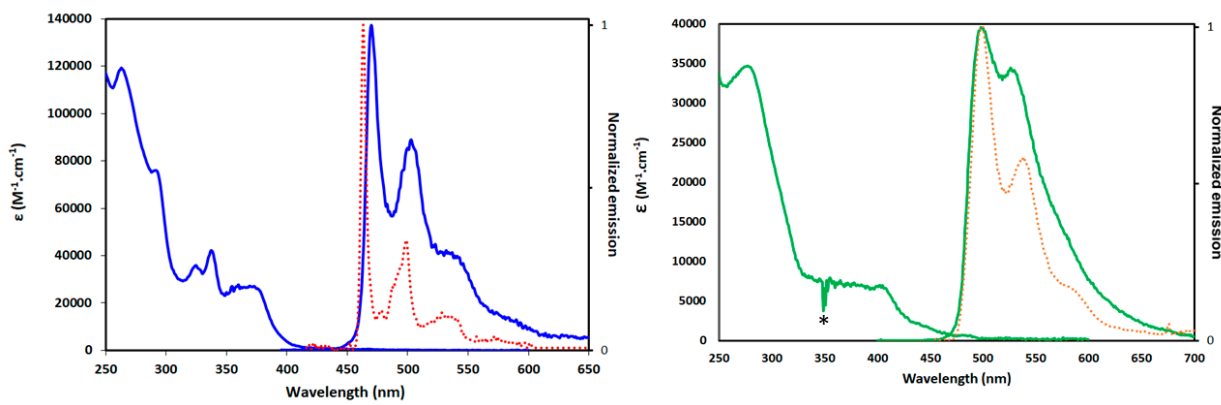


Figure 3. Absorption and emission spectra of **7** (left) and **8** (right) in a diluted solution in CH_2Cl_2 at 298 K (plain line) and 77 K emission spectra in butyronitrile (dotted line). * Artefact emanating from the spectrometer.

Table 2. Absorption and emission data recorded in CH_2Cl_2 at 298 K and in butyronitrile at 77 K.

Complexes	λ_{abs} [nm] ($\epsilon \times 10^3$ $\text{M}^{-1} \text{cm}^{-1}$)	λ_{em} [nm]	Φ (Air)	τ [μs] (Air)	$k_r \times 10^5$ [s^{-1}] ²	$\Sigma k_{\text{nr}} \times 10^5$ [s^{-1}] ²	$k[\text{O}_2] \times 10^9$ [$\text{M}^{-1} \text{s}^{-1}$] ³	λ_{em} [nm] 77 K	τ [μs] 77 K
$[\text{Ir}(\text{dpyx})(\text{ppy})\text{Cl}]$ ¹ [57]	258 (39.7), 285 (37.0), 353 (6.2), 369 (7.8), 399 (10.0), 417 (11.3), 455 (3.6), 492 (1.3),	508	0.76 (0.02)	1.6 (<0.10)	4.8	1.5	4.9	-	-
$[\text{Pt}(\text{dpb})\text{Cl}]$ [65]	-	493 *, 524, 560	0.49	3.4	1.4	1.4	-	-	-
7	262 (11.9), 293 (75.5), 314 (29.4), 327 (34.6), 339 (41.0), 349 (23.3), 368 (26.7), 403 (2.9), 440 (0.8)	470 *, 502, 533	0.18 (0.11)	1.6 (1.02)	1.1	5.1	0.2	463 *, 498, 538	2.3
8	254 (32.1), 280 (34.5), 400 (6.6), 440 (1.9), 484 (0.7)	505 *, 528	0.61 (0.10)	0.87 (0.12)	7.0	4.5	2.6	500 *, 538, 585	4.22

¹ This complex has been studied in CH_3CN . ² The rate constants for radiative (k_r) and nonradiative (Σk_{nr}) decay can be estimated from the quantum yields and lifetimes: $k_r = \Phi_{\text{lum}}/\tau$ and $\Sigma k_{\text{nr}} = (1/\tau)$. ³ Bimolecular rate constant for quenching by ${}^3\text{O}_2$, estimated from τ values in degassed and aerated solutions. * Denotes the most intense band.

Compound 8 displays a bright green structured emission with a maximum at 505 nm and a high quantum yield of 61%. The emission displays a lifetime of 0.87 μs , and both the lifetime and the quantum yield drop drastically in the presence of oxygen and the $k[\text{O}_2]$ is estimated to be $2.6 \times 10^9 \text{ M}^{-1} \text{s}^{-1}$. The shape of the emission spectrum is very similar to the model complex $[\text{Ir}(\text{dpyx})(\text{ppy})\text{Cl}]$, which displays a green structured emission with maximum at 508 nm and a quantum yield of 76%. However, the emission lifetime of $[\text{Ir}(\text{dpyx})(\text{ppy})\text{Cl}]$ is twice as long as that of 8 and much more sensitive to the presence of oxygen ($k[\text{O}_2] = 4.9 \times 10^9 \text{ M}^{-1} \text{s}^{-1}$). At 77 K, 8 displays a more pronounced structure for the

emission spectrum, but the emission maximum remains almost at the same wavelength (i.e., 500 nm) as at room temperature. The weak rigidochromism is indicative of an emission emanating from the radiative deactivation of the ligand centered (LC) triplet excited state [61,68], which is also the case for $[\text{Ir}(\text{dpyx})(\text{ppy})\text{Cl}]$. The two Ir^{III} complexes display very close emission properties despite the presence of the cyclometallating pyridine in 8.

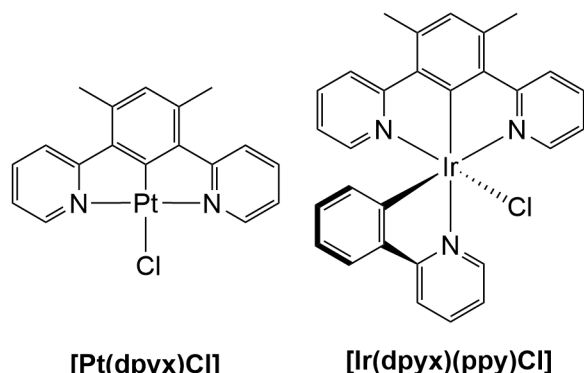


Figure 4. Reference complexes $[\text{Pt}(\text{dpyx})\text{Cl}]$ and $[\text{Ir}(\text{dpyx})(\text{ppy})\text{Cl}]$.

4. Conclusions

We successfully synthesized a dipyridylbenzene-like terdentate ligand featuring an electrodeficient cyclometallating ring; the ligand was fully characterized by NMR and HRMS. Two highly emissive neutral complexes were prepared: a Pt^{II} complex and a biscyclometallated trisheteroleptic Ir^{III} complex, emitting in the blue and in the green region of the spectrum, respectively. The Pt^{II} derivative required an unusual two step synthesis and some solubility issues interfered with its characterization. Nonetheless, we demonstrate that the introduction of the cyclometallating pyridine in the $\text{N}^{\text{C}}\text{N}$ ligand framework allows for inducing a significant hypsochromic shift of both the absorption and emission spectra with a good emission quantum yield (18%), and the emission is attributed to the radiative deactivation of a ${}^3\text{LC}^*$ to the ground state, as it is commonly encountered for this class of complexes. We believe this is a rare example of blue emitting Pt^{II} complex featuring a fluorine-free dipyridylbenzene-like terdentate ligand, which could be useful in optoelectronic devices [34,69]. In contrast, the Ir^{III} complex was obtained from an easier synthesis. The emission properties were found to be very close to those of the model complex $[\text{Ir}(\text{dpyx})(\text{ppy})\text{Cl}]$, with practically superimposable emission spectra. The emission is attributed to the radiative deactivation of a ${}^3\text{LC}^*$ to the ground state.

Supplementary Materials: The following supporting information containing the crystal structures determinations and refinements, and the NMR spectra can be downloaded at: <https://www.mdpi.com/article/10.3390/org4030029/s1>, Table S1: Crystal data and structure refinement; Figure S1: ^1H NMR Compound 1 in DMSO, 400 MHz; Figure S2: ^1H NMR Compound 2 in CDCl_3 , 400 MHz; Figure S3: ^1H NMR Compound 3 in CDCl_3 , 400 MHz; Figure S4: ^1H NMR Compound 4 in CDCl_3 , 400 MHz; Figure S5 ^1H NMR Compound 5 in CDCl_3 , 400 MHz; Figure S6: ^{13}C NMR compound 5 in CDCl_3 , 101 MHz; Figure S7: ^1H NMR Compound 6 in CDCl_3 , 400 MHz; Figure S8: ^{13}C NMR compound 6 in CDCl_3 , 101 MHz; Figure S9: ^1H NMR complex 7 in CD_2Cl_2 400 MHz; Figure S10: ^1H NMR complex 8 in CD_2Cl_2 500 MHz; Figure S11: ^{13}C complex 8 in CD_2Cl_2 126 MHz; Figure S12: Absorption spectra of compounds 7 (blue) and 8 (red) in CH_2Cl_2 at R.T. displaying the absorption band of the spin forbidden ${}^1\text{MLCT} \rightarrow {}^3\text{MLCT}$. References of the SI: Duisenberg, A. J. M., Kroon-Batenburg, L. M. J. & Schreurs, A. M. M. (2003). *J. Appl. Cryst.* 36, 220–229; Bruker (2004). SADABS. Bruker AXS Inc., Madison, Wisconsin, USA; Bruker (2005). XPREP. Bruker AXS Inc., Madison, Wisconsin, USA; Palatinus, L. & Chapuis, G. (2007). *J. Appl. Cryst.* 40, 786–790; Sheldrick, G. M. (2015). *Acta Cryst. C71*, 3–8; Dolomanov, O.V., Bourhis, L.J., Gildea, R.J., Howard, J.A.K. & Puschmann, H. (2009). *J. Appl. Cryst.* 42, 339–341.

Author Contributions: Conceptualization, P.-H.L.; methodology, P.-H.L.; formal analysis, P.-H.L. and F.L.; investigation, P.-H.L.; data curation, P.-H.L. and C.P.; writing—original draft preparation, P.-H.L. and F.L.; writing—review and editing, P.-H.L. and F.L.; project administration, P.-H.L.; funding acquisition, P.-H.L. All authors have read and agreed to the published version of the manuscript.

Funding: This work benefited from state aid managed by the National Research Agency under the “Investments for the future” and of the “Investissements d’avenir” program bearing the reference ANR-15-IDEX-02. This work was partially supported by CBH-EUR-GS (ANR-17-EURE-0003).

Acknowledgments: The authors thank the CNRS and Université de Grenoble Alpes for their support. The NanoBio ICMG (UAR 2607) is acknowledged for providing facilities for mass spectrometry (A. Durand, L. Fort, and R. Gueret), and single-crystal X-ray diffraction (N. Altounian).

Conflicts of Interest: The authors declare no conflict of interest.

References

- Li, T.-Y.; Wu, J.; Wu, Z.-G.; Zheng, Y.-X.; Zuo, J.-L.; Pan, Y. Rational Design of Phosphorescent Iridium(III) Complexes for Emission Color Tunability and Their Applications in OLEDs. *Coord. Chem. Rev.* **2018**, *374*, 55–92. [[CrossRef](#)]
- Pashaei, B.; Karimi, S.; Shahroosvand, H.; Abbasi, P.; Pilkington, M.; Bartolotta, A.; Fresta, E.; Fernandez-Cestau, J.; Costa, R.D.; Bonaccorso, F. Polypyridyl Ligands as a Versatile Platform for Solid-State Light-Emitting Devices. *Chem. Soc. Rev.* **2019**, *48*, 5033–5139. [[CrossRef](#)] [[PubMed](#)]
- Shon, J.H.; Teets, T.S. Molecular Photosensitizers in Energy Research and Catalysis: Design Principles and Recent Developments. *ACS Energy Lett.* **2019**, *4*, 558–566. [[CrossRef](#)]
- Zhao, Q.; Li, L.; Li, F.; Yu, M.; Liu, Z.; Yi, T.; Huang, C. Aggregation-Induced Phosphorescent Emission (AIPE) of Iridium(Iii) Complexes. *Chem. Commun.* **2008**, *3*, 685–687. [[CrossRef](#)] [[PubMed](#)]
- Solomatina, A.I.; Slobodina, A.D.; Ryabova, E.V.; Bolshakova, O.I.; Chelushkin, P.S.; Sarantseva, S.V.; Tunik, S.P. Blood-Brain Barrier Penetrating Luminescent Conjugates Based on Cyclometalated Platinum(II) Complexes. *Bioconjug. Chem.* **2020**, *31*, 2628–2637. [[CrossRef](#)]
- Costa, R.D.; Ortí, E.; Bolink, H.J.; Gruber, S.; Schaffner, S.; Neuburger, M.; Housecroft, C.E.; Constable, E.C. Archetype Cationic Iridium Complexes and Their Use in Solid-State Light-Emitting Electrochemical Cells. *Adv. Funct. Mater.* **2009**, *19*, 3456–3463. [[CrossRef](#)]
- Meier, S.B.; Tordera, D.; Pertegàs, A.; Roldà-Carmona, C.; Ortí, E.; Bolink, H.J. Light-Emitting Electrochemical Cells: Recent Progress and Future Prospects. *Mater. Today* **2014**, *17*, 217–223. [[CrossRef](#)]
- Salehi, A.; Fu, X.; Shin, D.-H.; So, F. Recent Advances in OLED Optical Design. *Adv. Funct. Mater.* **2019**, *29*, 1808803. [[CrossRef](#)]
- Zhao, J.H.; Hu, Y.X.; Lu, H.Y.; Lü, Y.L.; Li, X. Progress on Benzimidazole-Based Iridium(III) Complexes for Application in Phosphorescent OLEDs. *Org. Electron.* **2017**, *41*, 56–72. [[CrossRef](#)]
- Choy, W.C.H.; Chan, W.K.; Yuan, Y. Recent Advances in Transition Metal Complexes and Light-Management Engineering in Organic Optoelectronic Devices. *Adv. Mater.* **2014**, *26*, 5368–5399. [[CrossRef](#)]
- Lo, K.K.-W. Luminescent Rhodium(I) and Iridium(III) Polypyridine Complexes as Biological Probes, Imaging Reagents, and Photocytotoxic Agents. *Acc. Chem. Res.* **2015**, *48*, 2985–2995. [[CrossRef](#)]
- Yuan, Y.J.; Yu, Z.T.; Chen, D.Q.; Zou, Z.G. Metal-Complex Chromophores for Solar Hydrogen Generation. *Chem. Soc. Rev.* **2017**, *46*, 603–631. [[CrossRef](#)]
- Prier, C.K.; Rankic, D.A.; MacMillan, D.W.C. Visible Light Photoredox Catalysis with Transition Metal Complexes: Applications in Organic Synthesis. *Chem. Rev.* **2013**, *113*, 5322–5363. [[CrossRef](#)]
- Silvestroni, L.; Accorsi, G.; Armaroli, N.; Balzani, V.; Bergamini, G.; Campagna, S.; Cardinali, F.; Chiorboli, C.; Indelli, M.T.; Kane-Maguire, N.A.P.; et al. *Photochemistry and Photophysics of Coordination Compounds I*; Balzani, V., Campagna, S., Eds.; Springer: Berlin/Heidelberg, Germany, 2007; Volume 281, ISBN 9783642255281.
- Barbieri, A.; Barigelli, F.; Cheng, E.C.-C.; Flamigni, L.; Gunnlaugsson, T.; Kirgan, R.A.G.; Kumaresan, D.; Leonard, J.P.; Nolan, C.B.; Rillema, D.P.; et al. *Photochemistry and Photophysics of Coordination Compounds II*; Topics in current Chemistry; Campagna, S., Balzani, V., Eds.; Springer: Berlin/Heidelberg, Germany, 2007; ISBN 3-540-08986-1.
- Volman, D.H.; Hammond, G.S.; Neckers, D.C.; Maestri, M.; Balzani, V.; Deuschel-Cornioley, C.; Von Zelewsky, A. Photochemistry and Luminescence of Cyclometalated Complexes. *Adv. Photochem.* **1992**, *17*. [[CrossRef](#)]
- Gildea, L.F.; Williams, J.A.G. Iridium and Platinum Complexes for OLEDs. In *Organic Light-Emitting Diodes (OLEDs)*; Buckley, A., Ed.; Woodhead Publishing: Sawston, UK, 2013; pp. 77–113. ISBN 978-0-85709-425-4.
- Zanoni, K.P.S.; Coppo, R.L.; Amaral, R.C.; Murakami Iha, N.Y. Ir(III) Complexes Designed for Light-Emitting Devices: Beyond the Luminescence Color Array. *Dalton Trans.* **2015**, *44*, 14559–14573. [[CrossRef](#)] [[PubMed](#)]
- Housecroft, C.E.; Constable, E.C. Over the LEC Rainbow: Colour and Stability Tuning of Cyclometallated Iridium(III) Complexes in Light-Emitting Electrochemical Cells. *Coord. Chem. Rev.* **2017**, *350*, 155–177. [[CrossRef](#)]
- Kalinowski, J.; Fattori, V.; Cocchi, M.; Williams, J.A.G. *Light-Emitting Devices Based on Organometallic Platinum Complexes as Emitters*; Le Bozec, H., Guerchais, V., Eds.; Springer International Publishing: Berlin/Heidelberg, Germany, 2011; Volume 255.

21. Baranoff, E.; Yum, J.-H.; Jung, I.; Vulcano, R.; Grätzel, M.; Nazeeruddin, M.K. Cyclometallated Iridium Complexes as Sensitizers for Dye-Sensitized Solar Cells. *Chem. Asian J.* **2010**, *5*, 496–499. [[CrossRef](#)]
22. Guo, H.; Ji, S.; Wu, W.W.; Shao, J.; Zhao, J. Long-Lived Emissive Intra-Ligand Triplet Excited States (3IL): Next Generation Luminescent Oxygen Sensing Scheme and a Case Study with Red Phosphorescent Diimine Pt(II) Bis(Acetylide) Complexes Containing Ethynylated Naphthalimide or Pyrene Subunits. *Analyst* **2010**, *135*, 2832–2840. [[CrossRef](#)]
23. Medina-Rodríguez, S.; Denisov, S.A.; Cudré, Y.; Male, L.; Marín-Suárez, M.; Fernández-Gutiérrez, A.; Fernández-Sánchez, J.F.; Tron, A.; Jonusauskas, G.; McClenaghan, N.D.; et al. High Performance Optical Oxygen Sensors Based on Iridium Complexes Exhibiting Interchromophore Energy Shuttling. *Analyst* **2016**, *141*, 3090–3097. [[CrossRef](#)]
24. Lanoë, P.-H.; Le Bozec, H.; Williams, J.A.G.; Fillaut, J.-L.; Guerchais, V. Cyclometallated Platinum(II) Complexes Containing Pyridyl-Acetylide Ligands: The Selective Influence of Lead Binding on Luminescence. *Dalton Trans.* **2010**, *39*, 707–710. [[CrossRef](#)]
25. Lanoë, P.-H.; Fillaut, J.-L.; Toupet, L.; Williams, J.A.G.; Le Bozec, H.; Guerchais, V. Cyclometallated Platinum(II) Complexes Incorporating Ethynyl-Flavone Ligands: Switching between Triplet and Singlet Emission Induced by Selective Binding of Pb²⁺ Ions. *Chem. Commun.* **2008**, 4333–4335. [[CrossRef](#)] [[PubMed](#)]
26. Lanoë, P.-H.; Fillaut, J.-L.; Guerchais, V.; Le Bozec, H.; Williams, J.a.G. Metal Cation Induced Modulation of the Photophysical Properties of a Platinum(II) Complex Featuring a Dipicolylanilino–Acetylide Ligand. *Eur. J. Inorg. Chem.* **2011**, *2011*, 1255–1259. [[CrossRef](#)]
27. Ortega-Forte, E.; Hernández-García, S.; Vigueras, G.; Henarejos-Escudero, P.; Cutillas, N.; Ruiz, J.; Gandía-Herrero, F. Potent Anticancer Activity of a Novel Iridium Metallocdrug via Oncosis. *Cell. Mol. Life Sci.* **2022**, *79*, 510. [[CrossRef](#)]
28. Shen, J.; Rees, T.W.; Ji, L.; Chao, H. Recent Advances in Ruthenium(II) and Iridium(III) Complexes Containing Nanosystems for Cancer Treatment and Bioimaging. *Coord. Chem. Rev.* **2021**, *443*, 214016. [[CrossRef](#)]
29. Caporale, C.; Massi, M. Cyclometalated Iridium(III) Complexes for Life Science. *Coord. Chem. Rev.* **2018**, *363*, 71–91. [[CrossRef](#)]
30. Chung, C.Y.-S.; Yam, V.W.-W. Induced Self-Assembly of Platinum(II) Alkynyl Complexes through Specific Interactions between Citrate and Guanidinium for Proof-of-Principle Detection of Citrate and an Assay of Citrate Lyase. *Chemistry* **2014**, *20*, 13016–13027. [[CrossRef](#)]
31. Tu, T.; Fang, W.; Bao, X.; Li, X.; Dötz, K.H. Visual Chiral Recognition through Enantioselective Metallogel Collapsing: Synthesis, Characterization, and Application of Platinum-Steroid Low-Molecular-Mass Gelators. *Angew. Chem. Int. Ed.* **2011**, *50*, 6601–6605. [[CrossRef](#)]
32. Li, K.; Zou, T.; Chen, Y.; Guan, X.; Che, C. Pincer-Type Platinum(II) Complexes Containing N-Heterocyclic Carbene (NHC) Ligand: Structures, Photophysical and Anion-Binding Properties, and Anticancer Activities. *Chem. Eur. J.* **2015**, *21*, 7441–7453. [[CrossRef](#)]
33. Di Bella, C.S.; Dragonetti, M.; Pizzotti, D.; Roberto, F.; Tessore, R.; Ugo, M.G.; Humphrey, M.P.; Cifuentes, M.; Samoc, L.; Murphy, J.A.G.; et al. Molecular Organometallic Materials for Optics. *Top. Organomet. Chem.* **2010**, *37*, 179. [[CrossRef](#)]
34. Rausch, A.F.; Murphy, L.; Williams, J.A.G.; Yersin, H. Improving the Performance of Pt(II) Complexes for Blue Light Emission by Enhancing the Molecular Rigidity. *Inorg. Chem.* **2012**, *51*, 312–319. [[CrossRef](#)]
35. Congrave, D.G.; Hsu, Y.-T.; Batsanov, A.S.; Beeby, A.; Bryce, M.R. Sky-Blue Emitting Bridged Diiridium Complexes: Beneficial Effects of Intramolecular π–π Stacking. *Dalton Trans.* **2018**, *47*, 2086–2098. [[CrossRef](#)] [[PubMed](#)]
36. Culham, S.; Lanoë, P.-H.; Whittle, V.L.; Durrant, M.C.; Williams, J.A.G.A.G.; Kozhevnikov, V.N. Highly Luminescent Dinuclear Platinum(II) Complexes Incorporating Bis-Cyclometallating Pyrazine-Based Ligands: A Versatile Approach to Efficient Red Phosphors. *Inorg. Chem.* **2013**, *52*, 10992–11003. [[CrossRef](#)]
37. Lanoë, P.-H.; Tong, C.M.; Harrington, R.W.; Probert, M.R.; Clegg, W.; Williams, J.A.G.; Kozhevnikov, V.N. Ditopic Bis-Terdentate Cyclometallating Ligands and Their Highly Luminescent Dinuclear Iridium(III) Complexes. *Chem. Commun.* **2014**, *50*, 6831–6936. [[CrossRef](#)]
38. Ibrahim-Ouali, M.; Dumur, F. Recent Advances on Metal-Based near-Infrared and Infrared Emitting OLEDs. *Molecules* **2019**, *24*, 1412. [[CrossRef](#)]
39. Tamura, Y.; Hisamatsu, Y.; Kumar, S.; Itoh, T.; Sato, K.; Kuroda, R.; Aoki, S. Efficient Synthesis of Tris-Heteroleptic Iridium(III) Complexes Based on the Zn²⁺-Promoted Degradation of Tris-Cyclometalated Iridium(III) Complexes and Their Photophysical Properties. *Inorg. Chem.* **2017**, *56*, 812–833. [[CrossRef](#)]
40. Lepeltier, M.; Graff, B.; Lalevée, J.; Wantz, G.; Ibrahim-Ouali, M.; Gigmes, D.; Dumur, F. Heteroleptic Iridium (III) Complexes with Three Different Ligands: Unusual Triplet Emitters for Light-Emitting Electrochemical Cells. *Org. Electron. Phys. Mater. Appl.* **2016**, *37*, 24–34. [[CrossRef](#)]
41. Li, J.; Zhang, Q.; He, H.; Wang, L.; Zhang, J. Tuning the Electronic and Phosphorescence Properties of Blue-Emitting Iridium(Iii) Complexes through Different Cyclometalated Ligand Substituents: A Theoretical Investigation. *Dalton Trans.* **2015**, *44*, 8577–8589. [[CrossRef](#)] [[PubMed](#)]
42. Huckaba, A.J.; Cao, B.; Hollis, T.K.; Valle, H.U.; Kelly, J.T.; Hammer, N.I.; Oliver, A.G.; Webster, C.E. Platinum CCC-NHC Benzimidazolyl Pincer Complexes: Synthesis, Characterization, Photostability, and Theoretical Investigation of a Blue-Green Emitter. *Dalton Trans.* **2013**, *42*, 8820–8826. [[CrossRef](#)]
43. Darmawan, N.; Yang, C.-H.; Mauro, M.; Raynal, M.; Heun, S.; Pan, J.; Buchholz, H.; Braunstein, P.; De Cola, L. Efficient Near-UV Emitters Based on Cationic Bis-Pincer Iridium(III) Carbene Complexes. *Inorg. Chem.* **2013**, *52*, 10756–10765. [[CrossRef](#)]

44. Liu, Z.; Zhang, S.W.; Zhang, M.; Wu, C.; Li, W.; Wu, Y.; Yang, C.; Kang, F.; Meng, H.; Wei, G. Highly Efficient Phosphorescent Blue-Emitting [3+2+1] Coordinated Iridium(III) Complex for OLED Application. *Front. Chem.* **2021**, *9*, 758357. [[CrossRef](#)]
45. Sivasubramaniam, V.; Brodkorb, F.; Hanning, S.; Loebel, H.P.; van Elsbergen, V.; Boerner, H.; Scherf, U.; Kreyenschmidt, M. Fluorine Cleavage of the Light Blue Heteroleptic Triplet Emitter FIrpic. *J. Fluor. Chem.* **2009**, *130*, 640–649. [[CrossRef](#)]
46. Williams, J.A.G.; Beeby, A.; Davies, E.S.; Weinstein, J.A.; Wilson, C. An Alternative Route to Highly Luminescent Platinum(II) Complexes: Cyclometalation with N \wedge C \wedge N-Coordinating Dipyridylbenzene Ligands. *Inorg. Chem. Commun.* **2003**, *42*, 8609–8611. [[CrossRef](#)] [[PubMed](#)]
47. He, L.; Lan, Y.; Ma, D.; Song, X.; Duan, L. Fluorine-Free, Highly Efficient, Blue-Green and Sky-Blue-Emitting Cationic Iridium Complexes and Their Use for Efficient Organic Light-Emitting Diodes. *J. Mater. Chem. C* **2018**, *6*, 1509–1520. [[CrossRef](#)]
48. Wang, X.; Wang, S.; Pan, F.; He, L.; Duan, L. Cationic Iridium Complexes with 5-Phenyl-1H-1,2,4-Triazole Type Cyclometalating Ligands: Toward Blue-Shifted Emission. *Inorg. Chem.* **2019**, *58*, 12132–12145. [[CrossRef](#)]
49. Henwood, A.F.; Pal, A.K.; Cordes, D.B.; Slawin, A.M.Z.; Rees, T.W.; Momblona, C.; Babaei, A.; Pertegás, A.; Ortí, E.; Bolink, H.J.; et al. Blue-Emitting Cationic Iridium(III) Complexes Featuring Pyridylpyrimidine Ligands and Their Use in Sky-Blue Electroluminescent Devices. *J. Mater. Chem. C* **2017**, *5*, 9638–9650. [[CrossRef](#)]
50. Constable, E.C.; Henney, R.P.G.; Leese, T.A. Cyclometallation Reactions of 6-Phenyl-2,2'-Bipyridine; a Potential C,N,N-Donor Analogue of 2,2':6',2"-Terpyridine. Crystal and Molecular Structure of Dichlorobis(6-Phenyl-2,2'-Bipyridine)Ruthenium(II). *J. Chem. Soc. Dalton Trans.* **1990**, 443–449. [[CrossRef](#)]
51. Daniels, R.E.; Culham, S.; Hunter, M.; Durrant, M.C.; Probert, M.R.; Clegg, W.; Williams, J.A.G.; Kozhevnikov, V.N. When Two Are Better than One: Bright Phosphorescence from Non-Stereogenic Dinuclear Iridium(III) Complexes. *Dalton Trans.* **2016**, *45*, 6949–6962. [[CrossRef](#)]
52. Williams, J.A.G.; Develay, S.; Rochester, D.L.; Murphy, L. Optimising the Luminescence of Platinum(II) Complexes and Their Application in Organic Light Emitting Devices (OLEDs). *Coord. Chem. Rev.* **2008**, *252*, 2596–2611. [[CrossRef](#)]
53. Whittle, V.L.; Williams, J.A.G. A New Class of Iridium Complexes Suitable for Stepwise Incorporation into Linear Assemblies: Synthesis, Electrochemistry, and Luminescence. *Inorg. Chem.* **2008**, *47*, 6596–6607. [[CrossRef](#)]
54. Brouwer, A.M. Standards for Photoluminescence Quantum Yield Measurements in Solution (IUPAC Technical Report)*. *Pure Appl. Chem.* **2011**, *83*, 2213–2228. [[CrossRef](#)]
55. Błachut, D.; Wojtasiewicz, K.; Czarnocki, Z. Some Pyridine Derivatives as “Route-Specific Markers” in 4-Methoxyamphetamine (PMA) Prepared by the Leuckart Method: Studies on the Role of the Aminating Agent in Their Distribution in the Final Product. *Forensic Sci. Int.* **2005**, *152*, 157–173. [[CrossRef](#)]
56. Wilkinson, A.J.; Puschmann, H.; Howard, J.A.K.; Foster, C.E.; Williams, J.A.G. Luminescent Complexes of Iridium(III) Containing N⁺C≡N-Coordinating Terdentate Ligands. *Inorg. Chem.* **2006**, *45*, 8685–8699. [[CrossRef](#)]
57. Anderson, G.K.; Lin, M.; Sen, A.; Gretz, E. Reagents for Transition Metal Complexes and Oorganometallic Synthesis. In *Inorganic Syntheses*; Angelici, R.J., Ed.; John Wiley & Sons, Inc.: Hoboken, NJ, USA, 1990; Volume 28, pp. 1–463.
58. Kumaresan, D.; Shankar, K.; Vaidya, S.; Balzani, V.; Campagna, S.; Williams, J.A.G.; Francesco, P.; Bergamini, G.; Balzani, V.; Indelli, M.; et al. Photochemistry and Photophysics of Coordination Compounds: Platinum. In *Photochemistry and Photophysics of Coordination Compounds II*; Balzani, V., Campagna, S., Eds.; Springer: Berlin/Heidelberg, Germany, 2007; Volume 281, pp. 205–268. ISBN 978-3-540-73348-5.
59. Li, G.; Congrave, D.G.; Zhu, D.; Su, Z.; Bryce, M.R. Recent Advances in Luminescent Dinuclear Iridium(III) Complexes and Their Application in Organic Electroluminescent Devices. *Polyhedron* **2018**, *140*, 146–157. [[CrossRef](#)]
60. Williams, J.A.G. The Coordination Chemistry of Dipyridylbenzene: N-Deficient Terpyridine or Panacea for Brightly Luminescent Metal Complexes? *Chem. Soc. Rev.* **2009**, *38*, 1783–1801. [[CrossRef](#)] [[PubMed](#)]
61. Flamigni, L.; Barbieri, A.; Sabatini, C.; Ventura, B.; Barigelletti, F. Photochemistry and Photophysics of Coordination Compounds: Iridium. In *Photochemistry and Photophysics of Coordination Compounds II*; Springer: Berlin/Heidelberg, Germany, 2007; pp. 143–203.
62. Wilkinson, A.J.; Goeta, A.E.; Foster, C.E.; Williams, J.A.G. Synthesis and Luminescence of a Charge-Neutral, Cyclometalated Iridium(III) Complex Containing NCN- and CNC-Coordinating Terdentate Ligands. *Inorg. Chem.* **2004**, *43*, 6513–6515. [[CrossRef](#)]
63. Brulatti, P.; Gildea, R.J.; Howard, J.A.K.; Fattori, V.; Cocchi, M.; Williams, J.A.G. Luminescent Iridium(III) Complexes with N⁺C≡N-Coordinated Terdentate Ligands: Dual Tuning of the Emission Energy and Application to Organic Light-Emitting Devices. *Inorg. Chem.* **2012**, *51*, 3813–3826. [[CrossRef](#)] [[PubMed](#)]
64. Schulze, B.; Fribe, C.; Jäger, M.; Görls, H.; Birckner, E.; Winter, A.; Schubert, U.S. Pt(II) Phosphors with Click-Derived 1,2,3-Triazole-Containing Tridentate Chelates. *Organometallics* **2018**, *37*, 145–155. [[CrossRef](#)]
65. Rausch, A.F.; Homeier, H.H.H.; Yersin, H. *Organometallic Pt(II) and Ir(III) Triplet Emitters for OLED Applications and the Role of Spin–Orbit Coupling: A Study Based on High-Resolution Optical Spectroscopy*; Lees, A.J., Ed.; Springer: Berlin/Heidelberg, Germany, 2010.
66. Scattergood, P.A.; Ranieri, A.M.; Charalambou, L.; Comia, A.; Ross, D.A.W.; Rice, C.R.; Hardman, S.J.O.; Heully, J.-L.; Dixon, I.M.; Massi, M.; et al. Unravelling the Mechanism of Excited-State Interligand Energy Transfer and the Engineering of Dual Emission in [Ir(C≡N)₂(N⁺N)]⁺ Complexes. *Inorg. Chem.* **2020**, *59*, 1785–1803. [[CrossRef](#)]

67. Obara, S.; Itabashi, M.; Okuda, F.; Tamaki, S.; Tanabe, Y.; Ishii, Y.; Nozaki, K.; Haga, M. Highly Phosphorescent Iridium Complexes Containing Both Tridentate Bis(Benzimidazolyl)-Benzene or -Pyridine and Bidentate Phenylpyridine: Synthesis, Photophysical Properties, and Theoretical Study of Ir-Bis(Benzimidazolyl)Benzene Complex. *Inorg. Chem.* **2006**, *45*, 8907–8921. [[CrossRef](#)] [[PubMed](#)]
68. Lees, A.J. The Luminescence Rigidochromic Effect Exhibited by Organometallic Complexes: Rationale and Applications. *Comments Inorg. Chem. A J. Crit. Discuss. Curr. Lit.* **1995**, *17*, 319–346. [[CrossRef](#)]
69. Murphy, L.; Brulatti, P.; Fattori, V.; Cocchi, M.; Williams, J. a G. Blue-Shifting the Monomer and Excimer Phosphorescence of Tridentate Cyclometallated Platinum(II) Complexes for Optimal White-Light OLEDs. *Chem. Commun. (Camb)* **2012**, *48*, 5817–5819. [[CrossRef](#)] [[PubMed](#)]

Disclaimer/Publisher’s Note: The statements, opinions and data contained in all publications are solely those of the individual author(s) and contributor(s) and not of MDPI and/or the editor(s). MDPI and/or the editor(s) disclaim responsibility for any injury to people or property resulting from any ideas, methods, instructions or products referred to in the content.